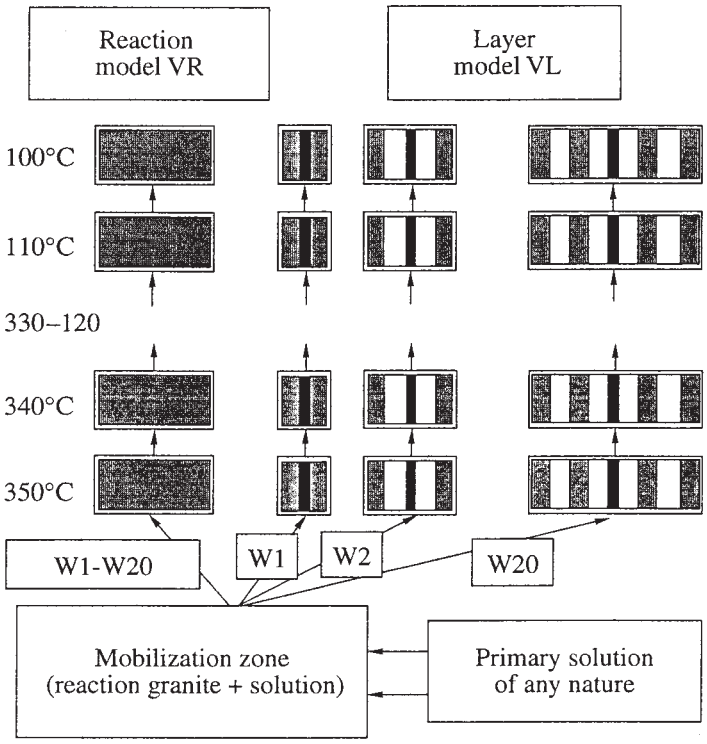

Fig. 61. Modeling scheme and model structures for the zone where filling veins are produced. W are waves of the solution from the mobilization zone, which are analogous to NF in Section 6.1.

any other source of S to maintain its high concentrations in the solution.

6.1.4. Conclusions

The equilibrium–dynamic modeling of the mobilization of ore components led us to establish the following:

(1) Interaction between primary barren solutions of any genesis and granites leads to the origin of metalliferous solutions, which can potentially be initial solutions for the hydrothermal system in question at elevated temperatures and pressures.

(2) Repeated interaction between barren hydrothermal fluids of constant composition with granites (at 310–420°C and 0.4–1.0 kbar) results in a significant increase in the concentrations of ore elements in the leaching solutions (up to $n \times 10^{-3}$ and $n \times 10^{-4}$ *m*) even without any changes in the external conditions.

(3) The metalliferous potential of the leaching solutions changes in the course of mobilization processes. Most of our models display the same unchanging leaching sequence of metals: the early stages of the process are dominated by the leaching of Zn, which is followed by Pb and Cu, i.e., Zn $\gg$ Pb $\geq$ Cu, and the solution becomes absolutely barren during the final stages of this process. A decrease in the pressure or sulfide sulfur content in the granite to 0.1–0.15 wt % partly impedes Cu extraction and results in the leaching succession Zn $\gg$ Pb > Cu.

(4) The concentration of S(II) in the leaching solutions ranges from $n \times 10^{-2}$ to $n \times 10^{-3}$ *m*, which fall within the range typical of medium-temperature hydrothermal deposits. These data demonstrate that there is no need to call upon other sources of sulfide sulfur for creating its realistic concentrations in the hydrothermal solution.

6.2. Model for the Genesis of Mineralized Veins

As was discussed above, the temperature gradients at our deposits can attain 20–40°C per 100 m updip the veins [Lyakhov *et al.*, 1978, 1994; Laz'ko *et al.*, 1981], and it can be hypothesized that a temperature decrease is one of the dominant factors of ore deposition. Proceeding from these facts and considerations, we model the changes in the equilibria in an ascending solution flow from the zone of metal mobilization in granite.

6.2.1. Simulation technique

The vein is modeled by a succession of 21–26 flow-through reactors (Fig. 61). Reactor 1 ("entrance" to the vein from below), into which the solution comes from the zone where metals are mobilized, has a temperature 20°C lower than the mobilization zone (350°C in most of our models, although we also analyzed other starting

temperatures in the range of 420 to 300°C). The temperature decreases by 10°C in every successive reactor. The pressure in the reactors was assumed to be constant and equal to 1 kbar in most of the models. We also explored models with a decreasing pressure in the zones of mobilization and ore deposition. The last reactor (upper "limit" of the vein) has a temperature of 100–150°C. Waves (portions) of the leaching solution from the mobilization zone successively pass through the reactors, in which thermodynamic equilibria are achieved, with the newly formed minerals remaining in the reactors and the equilibrium solution flowing to the next (updip) reactor. The calculations were carried out for 20–30 waves of the leaching solution coming from the mobilization zone. The number of waves (portions) of the solution can be regarded as a relative time scale.

In addition to the temperature effect on the origin of minerals, we also examined the dependences of mineral assemblages in filling veins on the composition of the country rocks (the rocks in the mobilization zone are the same as the rocks hosting the veins), the chemistry of the hydrothermal solutions (which enter into the mobilization zone of metals and produce a mineralized metalliferous solution of another composition), and reactions with the tectonized aluminosilicate material filling the fractures.

In the models we assumed *two extreme mechanisms producing filling veins* (Fig. 61). In one of the models, which can be referred to as the layer model and denoted VL, each portion (wave) of the hydrothermal solution coming from the mobilization zone passes separately through the reactors. The minerals formed when the previous waves passed through the reactor do not react with the newly coming wave of the hydrothermal solution from the mobilization zone. Hence, each portion of the hydrothermal solution produces its own equilibrium mineral association or a *layer* of these minerals. According to the other model, the *reaction* model VR, each successive portion (wave) of the solution from the mobilization zone reacts with the minerals that were formed in the vein by previous solution waves, and, thus, the preexisting minerals in the vein are completely transformed in the course of these reactions.

In addition to the two extreme mechanisms, we recently examined a few variants of intermediate *reaction–layer* models RL, in which a specified number of earlier layers can be reworked in each of the reactors [Borisov *et al.*, 2002]. The possibility of simulating such complicated models appeared after the development of a new version of the HCh program package [Shvarov, 1999; Shvarov and Bastarkov, 1999].

The realistic character of these models is validated by numerous lines of evidence, including our data (see Chapter 5) and information on the mineralogy of filling veins [Zlatogurskaya, 1960; Smirnov, 1978; Khetagurov *et al.*, 1986, 1992; Dobrovol'skaya, 1989].

6.2.2. Thermodynamic simulation results

The simulation results can be subdivided into six series.

1. Reference models VL1 and VR1 of mineral formation are based on the primary barren solution of basic model IS-2 (see Section 6.1).

The modeling conditions and parameters are as follows:

* in the mobilization zone, T = 370°C, P = 1 kbar, granite mass in the reactor is 10 kg (Kholst granite), the primary solution contains H_2CO_3 = 0.5 m, NaCl = 1.0 m, and HCl = 0.1 m; the reactor of the mobilization zone is successively passed by 20 portions or waves of the primary solution; the composition of the initial metalliferous solution was described in Section 6.1;

* in the developing filling vein, T = 350–100°C (the temperature step is 10°C), P = 1 kbar; minerals precipitate from homogeneous solutions in response to a temperature decrease in VL models and as a consequence of a temperature decrease and reactions with earlier vein minerals in VR models; the reactors are successively passed by 20 portions or waves of the initial ore-bearing solution from the mobilization zone (Fig. 51).

The calculation results are displayed in Figs. 62 and 63. The dominant minerals in both models are quartz (50–95% of the overall mass of the precipitated material), pyrite (0–50%), and, over some intervals, pyrrhotite.

The absence of interactions in model VL1 (Fig. 62) results in a fairly uniform distribution of ore minerals between the reactors. The highest temperature portions of the vein are dominated by Cu minerals (up to 2 wt % at wave 20), and the main ore mineral at 210–250°C is sphalerite. In the lower temperature region, the percentage of galena increases, and the content of this mineral become commensurable with that of sphalerite. The highest concentrations of galena and sphalerite (up to 5–6% each) are restricted to temperatures lower than 250°C. A characteristic structural feature of the vein is the preferable accumulation of sphalerite in layers 7–10 (precipitates from waves 7–10 of the metalliferous solution), in which the content of this mineral sometimes is high as 20–30% (at temperatures of 200°C or lower). Galena is distributed more uniformly between layers 11–20 and is contained in amounts of 10–15% at the same temperatures.

Our models thus reproduce the formation of quartz veins with Zn, Pb, and Cu sulfides and the evolution of the vein mineralogy updip (i.e., with temperature decrease) and with time (i.e., from wave to wave).

In reaction model VR-1 (Fig. 63), the distribution of ore material updip the vein is not uniform, and there are a number of intervals enriched in ore minerals. For example, sphalerite has two maxima of its precipitation at wave 10, at temperatures of above 300 and below 200°C; galena has two maxima at wave 20, one within the range of 250–300°C and the other at lower temper-

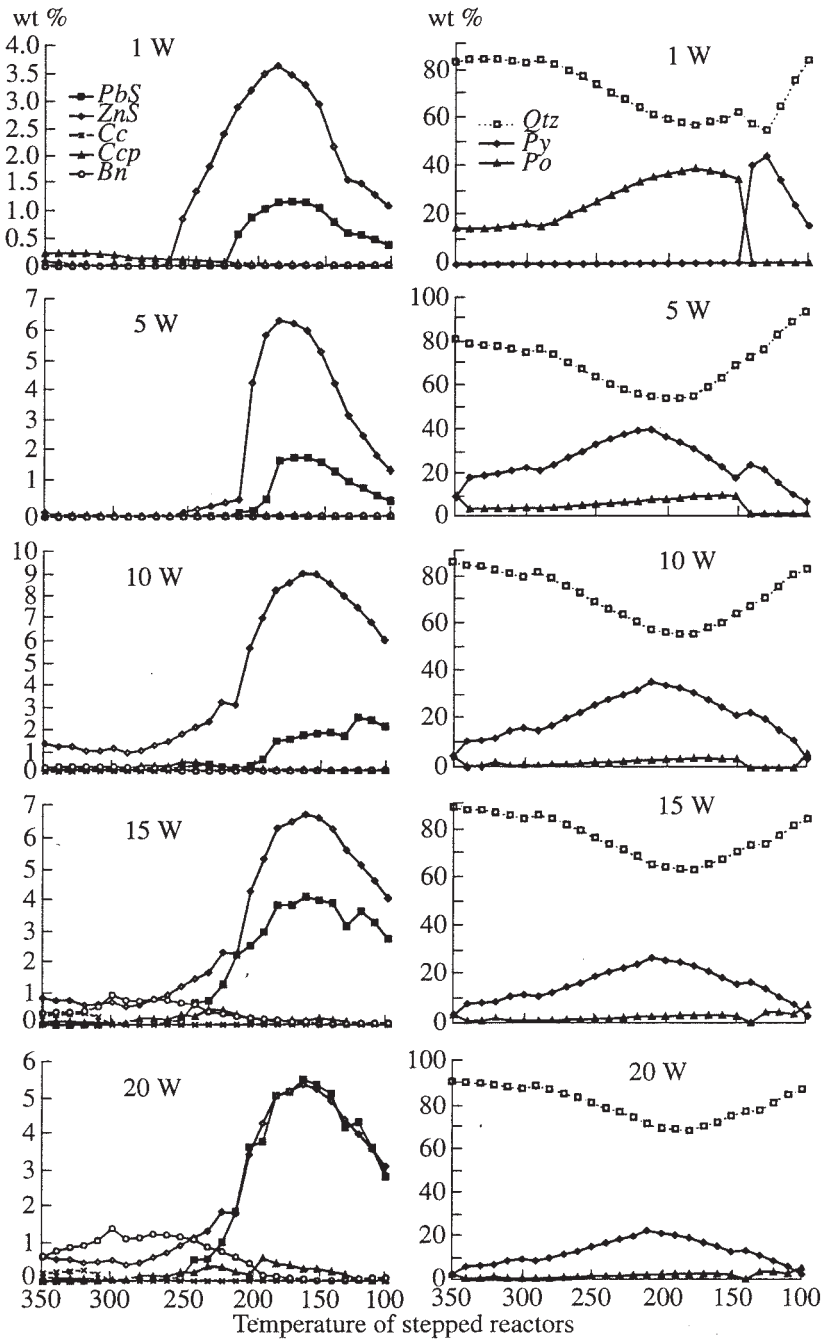

Fig. 62. Layer model VL1. The structure of the filling vein at waves 1, 5, 10, 15, and 20. Ore minerals (left-hand plots): *PbS*—galena, *ZnS*—sphalerite, *Ccp*—chalcopyrite, *Bn*—bornite, *Cc*—chalcocite; main gangue minerals (right-hand plots): *Qtz*—quartz, *Py*—pyrite, *Po*—pyrrhotite.

atures. It is worth noting that only at temperatures of 250–300°C is the galena content (8%) higher than the content of sphalerite (Fig. 63, wave 20).

Which of the two models is more plausible?

The parameter most suitable for comparing the models is the Pb/Zn ratio. At our deposits, this ratio varies from <1 in the lower parts of the veins to 1–2 and, rarely, up to 5 at their upper levels [Nekrasov, 1980; Lyakhov *et al.*, 1994; Dobrovol'skaya, 1989]. This criterion is met by the results of the layer model. The same ratio in the reaction model strongly increases downdip the veins (Fig. 63, a maximum of galena at high temperatures), which is obviously at variance with the factual data.

The layer model is capable of quite satisfactorily reflecting the stages of mineral precipitation described

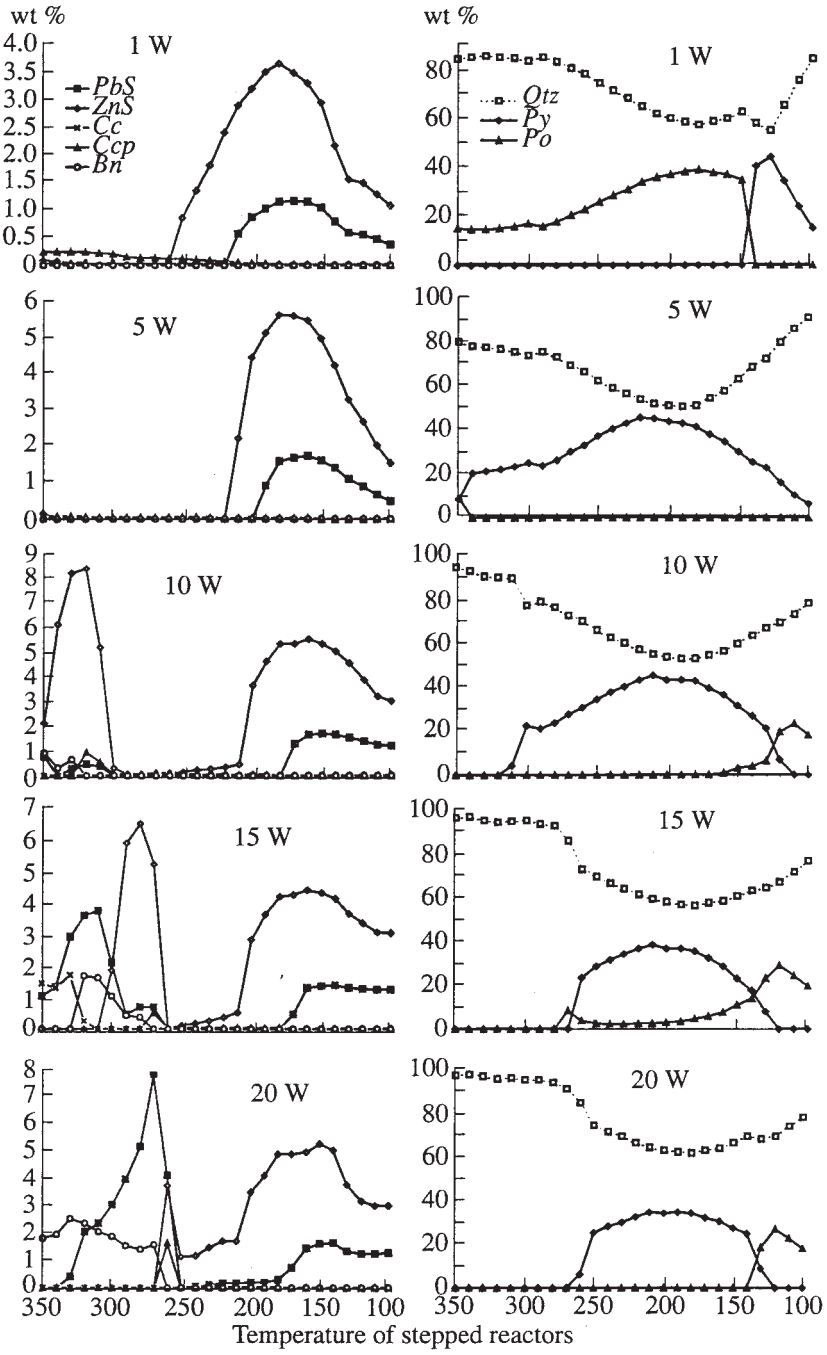

Fig. 63. Reaction model VR1. The structure of the filling vein at waves 1, 5, 10, 15, and 20. Ore minerals (left-hand plots): *PbS*—galena, *ZnS*—sphalerite, *Ccp*—chalcopyrite, *Bn*—bornite, *Cc*—chalcocite; main gangue minerals (right-hand plots): *Qtz*—quartz, *Py*—pyrite, *Po*—pyrrhotite.

at deposits of the Sadon group [Dobrovol'skaya, 1989]. The earliest mineral stage produced the quartz–pyrite–pyrrhotite assemblage. In the layer model, this corresponds to the initial stage in the development of the vein (waves 1–3), when the mineralized solution precipitates mostly quartz, pyrite, and pyrrhotite, and other minerals are present in strongly subordinate amounts. This stage is followed by the quartz–pyrite–sphalerite–pyrrhotite stage with variable proportions of sulfides and the occurrence of minor chalcopyrite amounts. In the layer model, this stage is satisfactorily correlated with the evolution of the vein during waves 5–8. Most economic mineral deposits are related to the quartz–galena–sphalerite association. This stage is characterized by an increase in galena precipitation, up to predominance of galena over sphalerite, and a decrease in

the amounts of pyrite. Similar relations in the model are characteristic of later evolutionary stages of the vein (waves 10–20) by the layer mechanism.

Natural observations are in good agreement with the data, calculated in compliance with the layer model, that the bulk of galena and sphalerite precipitate at 250–150°C (Fig. 62).

Based on the results of the comparison, all further models were developed based exclusively on the layer model for the genesis of filling veins.

For convenience of further analysis and comparison between the results, some data on the initial metalliferous solutions (which come into the zone of vein development from the mobilization zone) are presented in Table 39 for all models of ore formation in veins. These data on ore elements alone are displayed in separate plots before each model for vein ore formation.

2. Effect of pressure on mineral formation in veins: models VL2, VL2p, and VL10

Modeling conditions and parameters:

* In the mobilization zone, T = 370°C; the granite mass in the reactor is 10 kg (Kholst granite); the primary solution has the composition H_2CO_3 = 0.3 m, NaCl = 0.8 m, $CaCl_2$ = 0.1 m, and $NaHCO_3$ = 0.2 m (Table 39, IS-10); and the pressure is 1 kbar in VL2 and VL2p and 600 bar in VL10;

* In the developing filling vein, T = 350–150°C (the temperature step is 10°C); mineralization is formed in compliance with the layer mechanism; the pressure is 1 kbar in VL2, 600 bar in VL10, and variable (from 1000 bar to saturated water vapor pressure $P_{sat.\ vap.}$ with a step of 50 bar between reactors) in VL2p; and the compositions of the initial metalliferous solutions of the models are exhibited in Fig. 64.

In contrast to the reference model VL1, these and later models have other compositions of the primary and, correspondingly, metalliferous solutions (transition from the model of leaching IS-2 to IS-10, Fig. 64): this solution does not contain HCl; i.e., it is less acidic, but instead bears $CaCl_2$ and $NaHCO_3$, which is more consistent with data on inclusions. Figure 64 shows calculation data for the initial metalliferous solutions that are used in models VL2, VL2p, and VL10 for the genesis of mineralization in veins.

The precipitation of ore minerals in models at 1000 bar (VL2) and under a pressure gradient (VL2p) proceeds almost identically, except that in model VL2p, in which the temperature decrease is coupled with a decrease in the pressure, the variations in the solubility of minerals are of complicated character (a temperature decrease suppresses the solubility of ore minerals and, hence, is favorable for their precipitation, while pressure exerts the opposite effect). The proportions of gangue mineral in these models differ more significantly. For example, in the model with a pressure gradient, the amounts of precipitated pyrite and pyrrhotite are greater, but the maxima of their precipitation are shifted toward lower temperatures (5W for pyrite in VL2 at 230°C and lower and in VL2p at 210°C and lower, Figs. 65 and 66). As can be seen from Fig. 68, at practically equal sulfur concentrations in the model with a pressure gradient (VL2p), the iron concentration is notably higher in the low-temperature reactors than in the solutions of the model under 1000 bar (VL2). Generally, the effect of pressure gradient in the ore deposition zone is so insignificant that later models were constructed at a constant pressure.

It was demonstrated in the model for ore formation at 600 bar (VL10) that the initial metalliferous solution of the model (Fig. 64) under this pressure is characterized by a significant increase in the solubility of minerals and, consequently, ore elements are more rapidly extracted and transported to the region of vein origin. For example, Zn is completely extracted by six waves (by ten waves at 1000 bar), Pb by 14 waves (21 at 1000 bar), and Cu by 17 waves (22 at 1000 bar). The mobility of Pb relative to Cu increases, so that the last portions of the solution (waves 15–17) still contain Cu but no Pb, while both elements are removed almost synchronously at 1000 bar. These differences are also reflected in the precipitation of minerals in the vein. At 600 bar (model VL10, Fig. 67), the ore is richer in sphalerite, but the maximum of its deposition is shifted toward lower temperatures (the sphalerite concentration increases to 12–13% on waves 1–5 as compared to 3% in the model at 1000 bar), and, correspondingly, the fractions of galena and Cu sulfides decrease; the deposition of Fe sulfides also significantly increases (up to 50–60% during early ore deposition stages as compared to 20–30% in the model at 1000 bar), as is obvious from Fig. 68.

3. Effect of temperature on mineral formation in veins: models VL2, VL3, and VL5

Modeling conditions and parameters:

* In the mobilization zone, P = 1 kbar, the granite mass in the reactor is 10 kg (Kholst granite), the primary solution has a composition analogous to those in previous models (IS-10, Table 39), the reactor is successively passed by 20 portions or waves of the primary solution, and the temperature is 370°C for VL2, 440°C for VL3, and 320°C for VL5.

* In the region where the filling vein develops, the pressure is constant and equal to 1 kbar; mineralization is formed from homogeneous solutions only in compliance with the layer mechanism; and the temperature step is 10°C in all models, starting from 350 to 150°C in VL2, from 420 to 150°C in VL3, and from 300 to 150°C in VL5.

Figure 69 illustrates the compositions of the initial metalliferous solutions used in the models of mineral formation in veins. The model with a starting temperature of 420°C (440°C in the zone of metal mobilization) shows the fastest extraction of metals from the granite compared with that in the model for 350°C (i.e., compared with VL2, Fig. 65). It was demonstrated that Zn

Table 39. Initial metalliferous solutions in the models of mineral formation in veins

Components of the metalliferous solution	Model vein no. (Fig ....)													
	VL1 (Fig. 62), VR1 (Fig. 63)		VL2 (Fig. 65), VL2p (Fig. 66)*, VL6 (Fig. 74)		VL3 (Fig. 70)		VL10 (Fig. 67)		VL5 (Fig. 71)		VL4 (Fig. 73)		VL9 (Fig. 76)	
	Mobilization model for this vein model, index (Fig. ...)													
	IS-2 (Fig. 51)		IS-10 (Fig. 64)		IS-10 (Fig. 69)		IS-10 (Fig. 64)		IS-10 (Fig. 69)		IS-2s (Fig. 72)		IS-27 (Fig. 75)	
	370°C, 1000 bar		370°C, 1000 bar		440°C, 1000 bar		370°C, 600 bar		320°C, 1000 bar		370°C, 1000 bar		370°C, 1000 bar	
	*1***		*2*										*3*	
	waves													
	1	10	1	10	1	10	1	10	1	10	1	10	1	10
K	1.99e–1	2.01e–1	1.80e–1	1.81e–1	2.24e–1	2.26e–1	1.84e–1	1.86e–1	1.37e–1	1.39e–1	2.00e–1	2.01e–1	1.80e–1	1.81e–1
Na	8.78e–1	8.81e–1	8.01e–1	8.00e–1	7.42e–1	7.45e–1	7.85e–1	7.87e–1	8.38e–1	8.46e–1	8.85e–1	8.83e–1	8.01e–1	8.02e–1
Ca	9.83e–3	6.70e–3	8.18e–3	6.79e–3	3.96e–3	4.29e–3	1.09e–2	9.08e–3	1.32e–2	8.96e–3	6.09e–3	6.62e–3	7.96e–3	5.38e–3
Mg	1.91e–5	2.69e–5	1.55e–5	1.92e–5	5.49e–5	6.11e–5	3.21e–5	4.01e–5	1.14e–5	1.66e–5	2.54e–5	2.73e–5	1.57e–5	2.19e–5
Al	4.19e–5	3.88e–5	4.25e–5	3.95e–5	9.41e–5	8.71e–5	3.29e–5	3.05e–5	2.20e–5	2.02e–5	4.21e–5	3.88e–5	4.29e–5	3.98e–5
Si	2.26e–2	2.09e–2	2.24e–2	2.10e–2	3.41e–2	3.17e–2	1.91e–2	1.79e–2	1.56e–2	1.45e–2	2.25e–2	2.09e–2	2.26e–2	2.12e–2
Fe	4.50e–3	4.34e–3	3.75e–3	3.74e–3	1.89e–2	2.05e–2	8.55e–3	8.63e–3	1.25e–3	1.22e–3	4.05e–3	4.34e–3	3.72e–3	3.55e–3
Cl	1.1	1.1	1.0	1.0	1.0	1.0	1.0	1.0	1.0	1.0	1.1	1.1	1.0	1.0
C	0.5	0.5	0.5	0.5	0.5	0.5	0.5	0.5	0.255	0.390	0.5	0.5	0.3	0.3
Zn	1.81e–4	6.01e–4	1.29e–4	1.64e–3	4.06e–3	–	6.54e–4	–	1.33e–5	1.51e–5	1.66e–4	2.00e–4	1.27e–4	1.61e–3
Pb	1.68e–5	8.19e–5	1.61e–5	2.96e–5	6.92e–5	–	2.42e–5	2.83e–4	5.29e–6	5.27e–6	1.83e–5	1.76e–5	1.63e–5	3.04e–5
Cu	1.27e–5	1.68e–4	1.17e–5	8.46e–5	1.90e–5	–	1.07e–5	2.76e–4	3.01e–6	5.54e–7	2.12e–6	2.23e–6	1.07e–5	7.41e–5
S	2.16e–2	8.17e–4	2.15e–2	1.74e–3	5.86e–2	–	2.83e–2	4.22e–4	1.00e–2	9.73e–3	2.43e–2	2.26e–2	2.18e–2	1.70e–3
pH	5.324	5.304	5.35	5.332	5.414	5.397	5.38	5.361	5.401	5.376	5.323	5.304	5.351	5.331
Ionic strength	0.6324	0.669	0.585	0.618	0.418	0.438	0.529	0.559	0.701	0.745	0.632	0.67	0.584	0.618

*Model with a pressure gradient in the region of vein mineral formation; ** primary solutions: (*1*) H_2CO_3 = 0.5 *m*, NaCl = 1.0 *m*; HCl = 0.1 *m*; (*2*) H_2CO_3 = 0.3 *m*, NaCl = 0.8 *m*; $CaCl_2$ = 0.1 *m*, $NaHCO_3$ = 0.2 *m*; (*3*) H_2CO_3 = 0.2 *m*, NaCl = 0.8 *m*; KCl = 0.2 *m*, $NaHCO_3$ = 0.2 *m*.

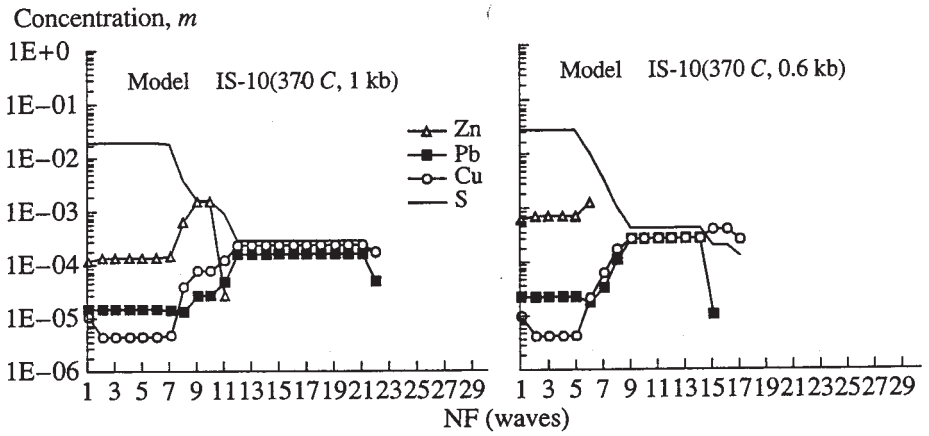

Fig. 64. Initial metalliferous solutions in ore-formation models VL2—1000 bar, VL2p—pressure gradient, VL10—600 bar. The variations in the concentrations (logarithms of molality) of ore elements and sulfide sulfur in the metalliferous solution at different portions (waves) of the primary solution.

is fully extracted here by two interaction waves, Pb by six waves, and Cu by seven waves (Fig. 69). Correspondingly, sulfides are precipitated in the vein (Fig. 70). The first two to three waves deposit the bulk of pyrite, pyrrhotite, sphalerite, and their contents in the vein material precipitated over this time span amounts to 75, 65, and 35 wt %, respectively. Such high contents of iron sulfides and sphalerite were obtained in none of our other models. As the process evolves further (i.e., at a greater number of waves), galena and Cu minerals precipitate (in amounts of up to 4–5% and 1.5%, respectively), along with the bulk of gangue quartz. A disadvantage of the model is the uneven distribution of ZnS and the inconsistency of the model with the normal vertical zoning of the deposit, i.e., a decrease in the Pb/Zn ratio.

The model with a starting temperature of the solution that enters the vein of 300°C (320°C in the mobilization zone, Fig. 69) is noted for the very "slow" removal of elements (because of a decrease in the solubility with decreasing temperature), so that even the passage of as many as 30 waves through the mobilization zone extracts only part of Zn, Pb, and Cu from the granite (Fig. 69). Consequently, the developing vein (or its segment) contains no more than 0.2–0.4% sulfides (Fig. 71).

The analysis of the simulation results of models with different temperatures reveals an important regularity: the higher the temperature in the mobilization zone, the lower the temperature at which ore sulfides start to precipitate in the vein. For example, sphalerite begins to precipitate starting from 240°C in the "hottest" model (VL3), from 270–280°C in the reference model (VL2), and from 290–300°C in the "coolest" model (VL5). The main sulfides with the highest solubility and characterised by the highest contents are iron sulfides (pyrrhotite and pyrite). The deposition of these minerals starts at the highest temperatures, with the reaction proceeding as

$$FeCl_2 + H_2S = FeS + 2HCl \quad (6.1)$$

The precipitation of 1 mole of pyrrhotite brings about the formation of 2 moles of HCl, and, inasmuch as the concentration of Fe complexes is much higher than the concentration of Zn complexes, pyrrhotite (pyrite) deposition impedes sphalerite deposition:

$$ZnCl_2 + H_2S = ZnS + 2HCl \quad (6.2)$$

Since the solubility of sulfides is at a maximum at the highest temperature and, hence, the solution produced at 440°C contains the highest concentrations of Fe and S, the solution acidity that hampers sphalerite precipitation is maintained here at lower temperatures than in models with temperatures of 370 and 300°C in the mobilization area.

It follows that, significantly affecting the process of mobilization of components, temperature gives rise to differences in the deposition of vein iron sulfides. These sulfides largely control the behavior of base-metal sulfides: pyrite and pyrrhotite precipitation significantly acidifies the solution, which, in turn, notably hampers the deposition of sphalerite, galena, and copper sulfides.

4. Effect of the sulfur content in the rocks of the mobilization zone on the vein structure: models VL1 and VL4

As was demonstrated above (see Section 6.1), the small variations in the sulfide sulfur concentration of the source granite may result in leaching solutions with strongly subordinate concentrations of copper (Fig. 54). We used the models of this group to test the effect of an increase in the S concentration of the granite on the deposition of minerals in the vein. For this purpose we constructed model VL4, whose parameters are analogous to those of model VL1 (Fig. 62) except for the

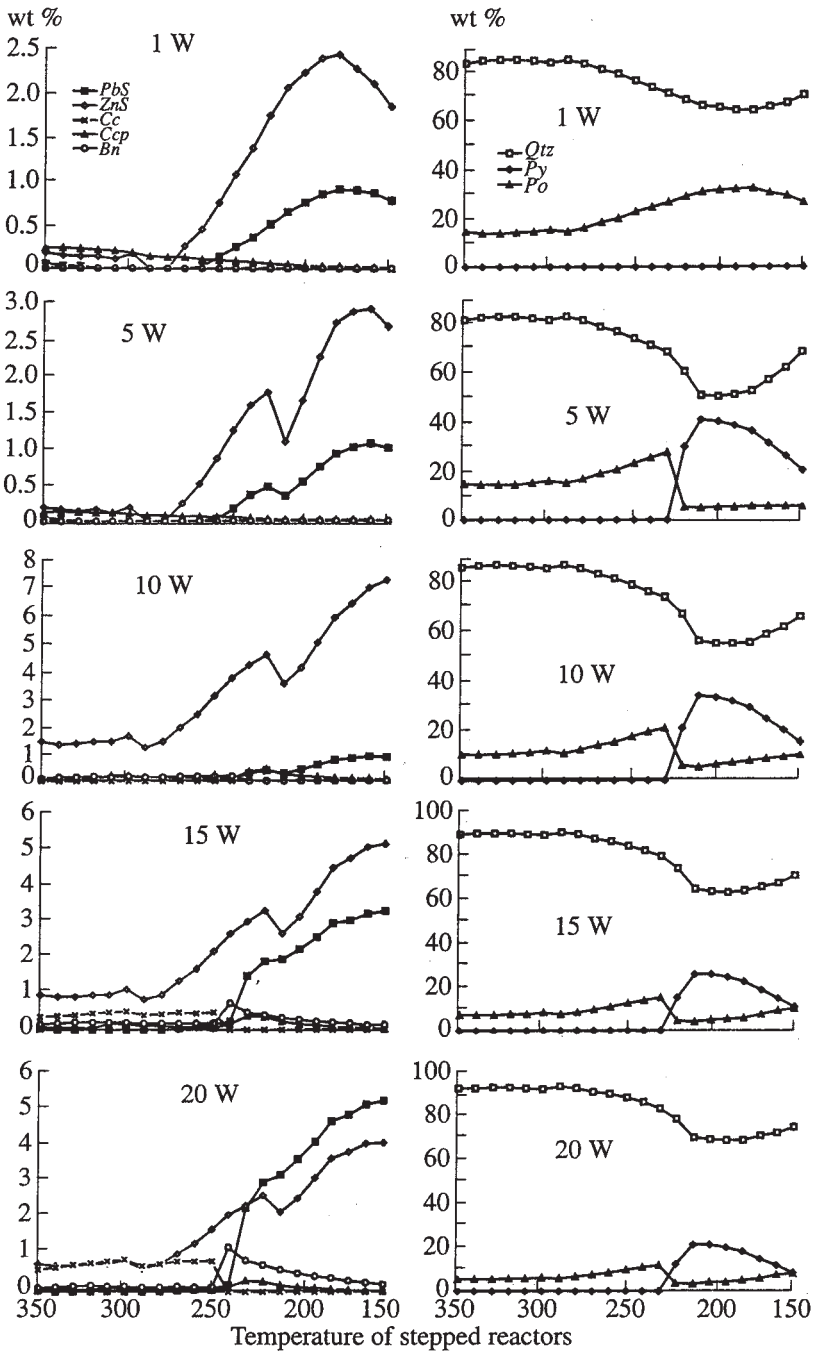

Fig. 65. Layer model VL2 of ore formation (P = const = 1 kbar). The structure of the filling vein at waves 1, 5, 10, 15, and 20 (the initial metalliferous solution in Fig. 64 is as according to leaching model IS-10).

granite composition only. To explore the specific effect of S but not of other components, we took two compositions of granite from the Kholst deposit (Table 35) that differed only in S contents (part of Fe was recalculated from the oxide to sulfide mode): 0.06 wt % S in model VL1 (or 0.016 gram atom of S per 1 kg of granite) and 0.14 wt % S in new model VL4 (or 0.044 gram atom of S per 1 kg of granite).

Modeling conditions and parameters:

P = 1 kbar, the granite mass in the reactor is 10 kg, the primary solution has a composition analogous to that in model VL1 (leaching model IS-2), the temperature in the mobilization zone is 370°C, and the temperature step is 10°C; i.e., the temperature decreases in both models from 350 to 100°C.

Figure 72 portrays the calculation data for the leaching solutions of model IS-2s at 370°C during the reac-

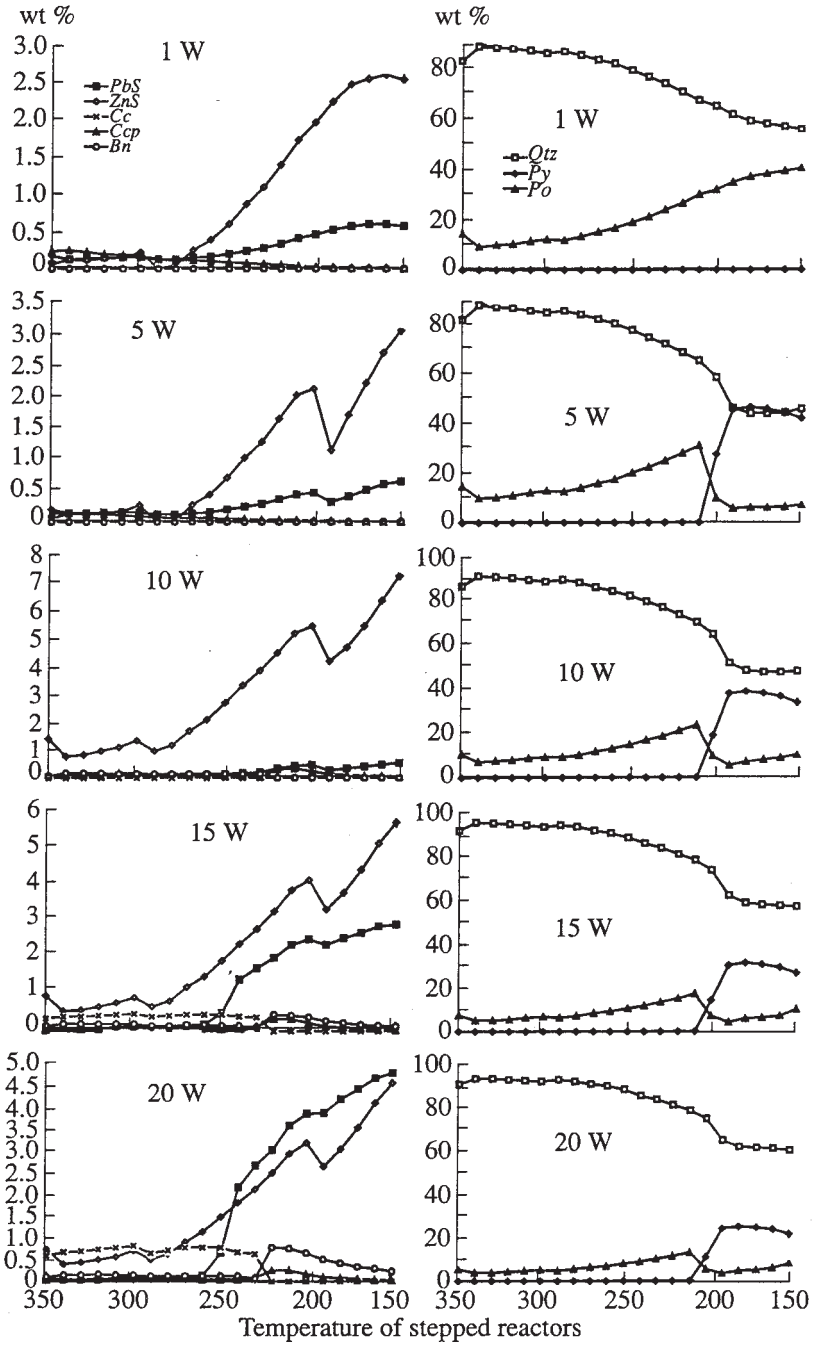

Fig. 66. Layer model VL2p of ore formation (*P* changes from 1000 bar to saturated water vapor pressure with a step of 50 bar between reactors; i.e., a temperature decrease by 10°C corresponds to a pressure decrease by 50 bar). The structure of the filling vein at waves 1, 5, 10, 15, and 20 (initial metalliferous solution in Fig. 64 is as according to leaching model IS-10).

tion with granite bearing an elevated concentration of sulfide sulfur (which was assumed as model VL4).

A distinctive feature of the mobilization process is a high concentration of sulfide sulfur maintained in the solution over 14 waves because of the relatively high sulfur content in the starting granite. This decelerates the leaching of ore elements and almost completely suppresses the extracting of Cu (at least over 30 waves).

The composition of the filling vein produced by these solutions is shown in Fig. 73, which illustrates the following characteristic feature of ore formation in this situation: the only Fe sulfide produced in this model (VL4) is pyrite, while the reference model (VL1) is characterized by the deposition of up to 40% pyrrhotite during the first few waves (Fig. 62). Sphalerite precipitates at the lowest temperatures among those in all models: 220°C (in model VL1 sphalerite starts to form

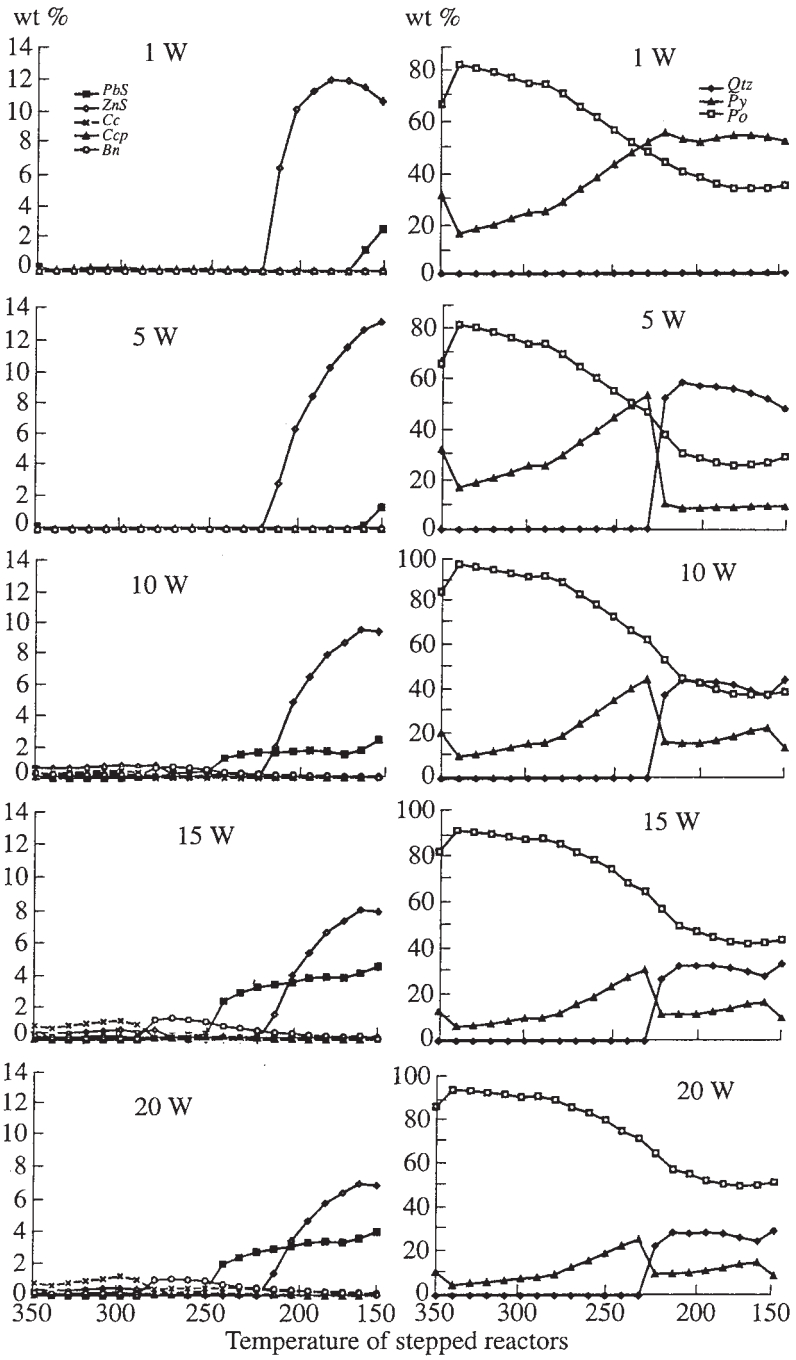

Fig. 67. Model VL10 of ore formation (P = const = 600 bar). The structure of the filling vein at waves 1, 5, 10, 15, and 20 (initial metalliferous solution in Fig. 64 is as according to leaching model IS-10).

at 250–260°C). Copper minerals are virtually absent. The Pb/Zn ratio is lower than one throughout the whole ore formation interval.

5. Effect of the ore deposition environment on the vein composition: models VL6 and VL7

All of our previous models have dealt with the deposition of mineral precipitate in the open fracture space (even in the "reaction" model VR1, the primary ore formation takes place in an "empty" fracture). However, at the deposits discussed here, veins often contain fragments of the strongly altered wall rocks, and, hence, it is highly probable that the ore mineralization was deposited when the metalliferous solutions interacted with the disintegrated and crushed material of the country rocks (which will be referred to below as clastic material).

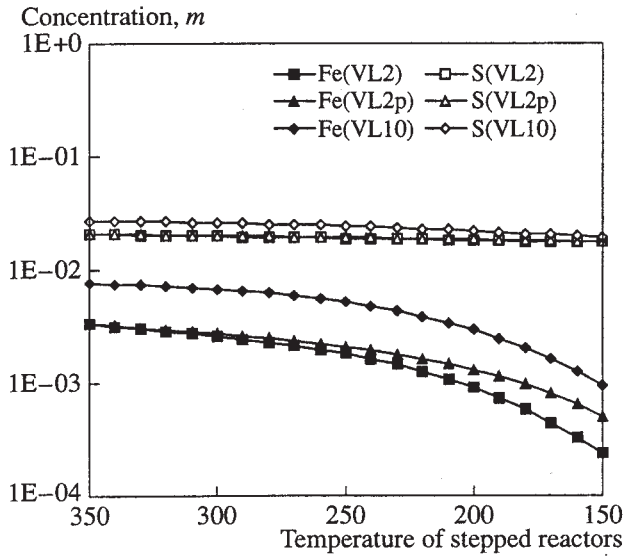

Fig. 68. Equilibrium Fe and S(II) concentrations in the solution in stepped reactors of vein models for P = 1000 bar (VL2), a pressure gradient (VL2p), and P = 600 bar (VL10) during the first stage (wave) of the origin of the filling vein.

In order to clarify the effect of the clastic material on the formation of ore mineralization, we introduced material of granitic composition into the reactors modeling the vein: 0.1 g (in each reactor and each wave) in model VL6 and 1 g (in each reactor and each wave) in model VL7. All other parameters of the models were analogous to those of model VL2.

The calculation results for model VL6 are shown in Fig. 74. Compared with model VL2, the effect of clastic material on the vein formation is manifested as follows: (1) the overall content of ore minerals in the precipitated vein material decreases (for example, the maximum content of sphalerite does not exceed 2%); (2) ore sulfides begin to be deposited at higher temperatures (starting from 350°C); and (3) muscovite and kaolinite crystallize in the vein, and their contents attain 25–35%.

Models VL6 and VL7 show significant differences. For example, kaolinite is not formed in model VL7, and muscovite is stable throughout the whole temperature range. Another characteristic feature of model VL7 is chlorite formation: Fe-chlorite predominates during the early stages of vein evolution, and Fe–Mg chlorite is widespread (up to 5–7%) during the late stages.

There are some differences between the distributions of ore sulfides updip the vein: in the model with a lower content of clastic material (VL6), the maximum of sphalerite precipitation is restricted to the highest temperatures, while the maximum of galena formation occurs at the lowest temperatures; in the model with a higher content of clastic material (VL7), all ore minerals are precipitated at high temperatures. This is caused, on the one hand, by the occurrence of sulfide sulfur in the solution in concentrations sufficient for the deposition of sulfides at alkalization, and, on the other hand, by reactions with the clastic material, which induce this alkalization (for example, at wave 1 in models VL6 and VL7: at T = 350°C, pH 5.05 and 5.23, respectively, at 300°C pH 4.54 and 5.25, and at 150°C pH 3.63 and 4.66). As can be seen from Fig. 74, even insignificant variations in the amount of the clastic material introduced into the reaction can significantly modify the process of mineral formation.

In addition to reactions with the clastic material in shear fractures, it is interesting to examine metasomatic reactions in the vein. Base-metal ores at the deposit overprint numerous iron sulfides, and the early pyrrhotite and pyrite are quite often corroded by ore sulfides. As follows from our calculations, when metalliferous solutions affect pyrite or pyrrhotite in the models,

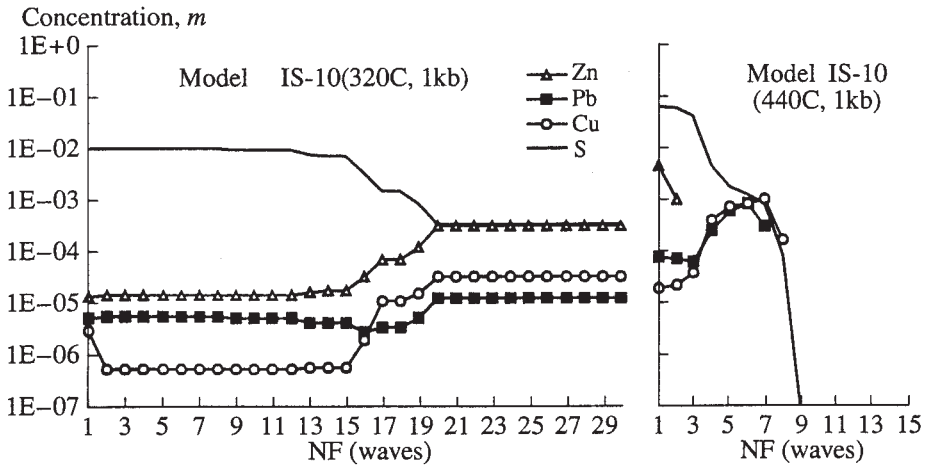

Fig. 69. Initial metalliferous solutions of ore-formation models VL5 (from 320°C) and VL3 (from 440°C). Variations in the concentrations (logarithm of molality) of ore elements and sulfide sulfur in the metalliferous solution are functions of the number of the primary solution portion (wave).

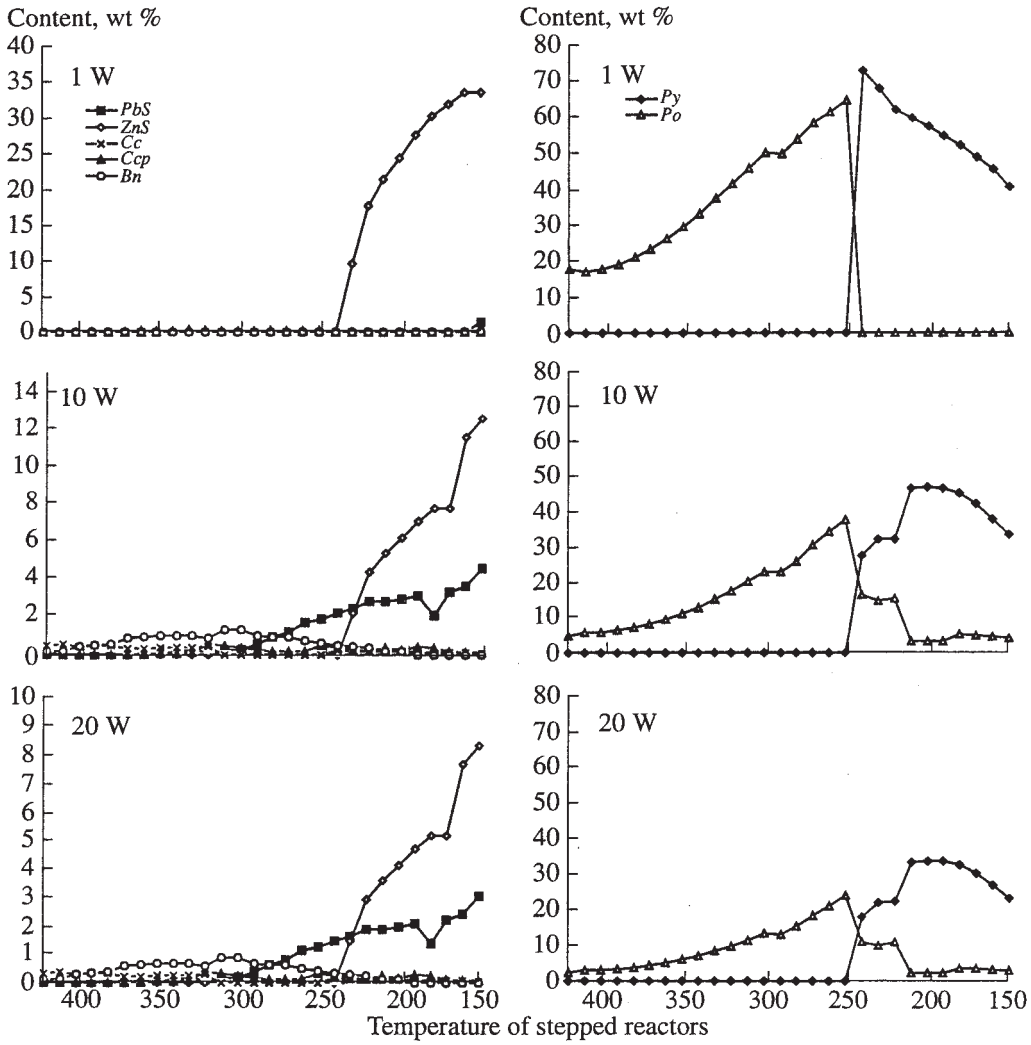

Fig. 70. VL3 model at 420°C at the "entrance" to the zone of vein formation (440°C in the mobilization zone, P = 1000 bar). The structure of the filling vein at waves 1, 10, and 20 (initial metalliferous solution in Fig. 69). Quartz is not shown in the right-hand plots, and the concentration of this mineral is complementary to 100%.

sphalerite, galena, and chalcopyrite are completely deposited because of reactions with the iron sulfides. Examples of such in-vein metasomatism can be demonstrated by reaction model VR1 (Fig. 63).

6. Effect of the composition of the primary barren solution on ore deposition: models VL1, VL2, and VL9

The effect of compositional variations of the primary barren solution on ore deposition in the vein can be traced in three models, two of which (VL1 and VL2) were discussed above (Figs. 62, 65), and VL9 is an additional model.

The differences between the models are as follows:

VL1—initial metalliferous solutions (Fig. 51) (primary solution: H_2CO_3 = 0.5, NaCl = 1.0, and HCl = 0.1 *m*);

VL2—initial metalliferous solutions (Fig. 64) (primary solution: H_2CO_3 = 0.3, NaCl = 0.8, $CaCl_2$ = 0.1, and $NaHCO_3$ = 0.2 *m*);

VL9—initial metalliferous solutions (Fig. 75) (primary solution: H_2CO_3 = 0.1, NaCl = 0.8, KCl = 0.2, and $NaHCO_3$ = 0.2 *m*).

All other parameters of the models are analogous.

Figure 75 presents the calculation results for the solutions of leaching model IS-27 (based on mineral formation in vein according to VL9), and Fig. 76 exhibits the results for model VL9 of vein development.

Comparison of the models with different compositions of their primary barren solutions demonstrates (Figs. 62, 65, and 76) that the resulting veins are generally quite similar but show some differences. The Pb/Zn ratio in model VL2 becomes greater than 1 at temperatures of 220° or lower, and the same ratio is equal to 1 in model VL1 and <1 in model VL9. The cause of this phenomenon can be revealed by comparing the models for mobilization and models for vein development. For example, in model IS-27 (Fig. 75, leaching model for

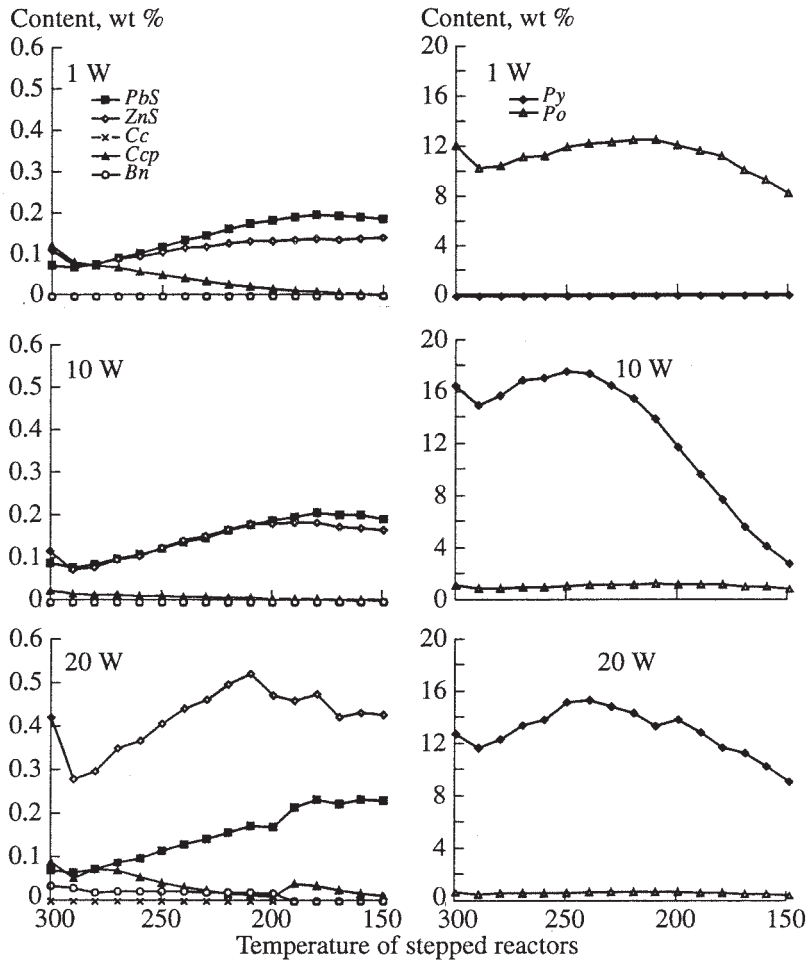

Fig. 71. VL5 model at 300°C at the "entrance" to the zone of vein formation (320°C in the mobilization zone, P = 1000 bar). The structure of the filling vein at waves 1, 10, and 20 (initial metalliferous solution in Fig. 69). Quartz is not shown in the right-hand plots, and the content of this mineral is equal to 80–90%.

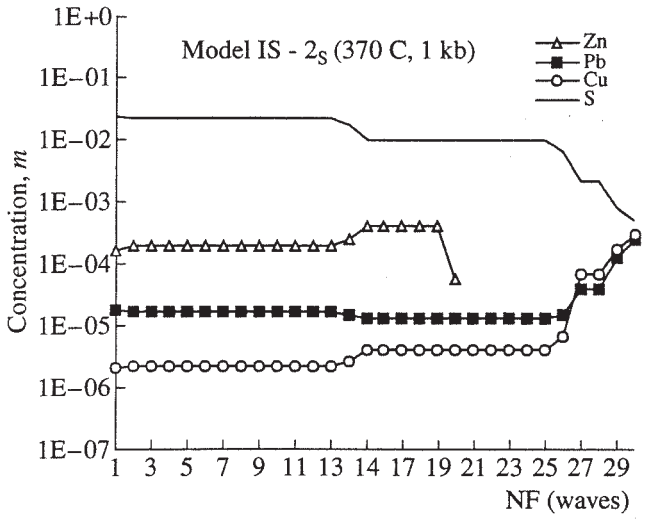

Fig. 72. Initial metalliferous solution of ore-formation model VL4 (mobilization model IS-2*s*, 370°C, 1 kbar, 1 kg of the Kholst granite with an elevated sulfur content).

VL9), Zn mobilization is much faster than Pb and Cu mobilization, so that the 20 waves used in our simulations can extract only part of Pb and Cu. The mobilization scenarios in models VL1 and VL2 are similar, and the differences between the deposition of sphalerite and galena arise due to the higher Cl concentration in the primary solution of model VL1. Because of this, sphalerite starts to precipitate in model VL2 at a higher temperature, and, by wave 20, the maximum of its content does not exceed 4%, whereas the galena concentrations in both models are close to 5%.

7. The reaction–layer models of mineral formation: RL are based on the barren primary solution of model IS-2. The calculations were conducted for 30–40 waves of the leaching solution, which came from the mobilization zone and recycled 1, 2, 5, and 10 preexisting layers in each reactor at each wave. The results are compared with those of reference models VL1 and VR1.

The main tendencies in the updip changes in the ore mineralogy are as follows: (1) the region where galena precipitation predominates over that of sphalerite is

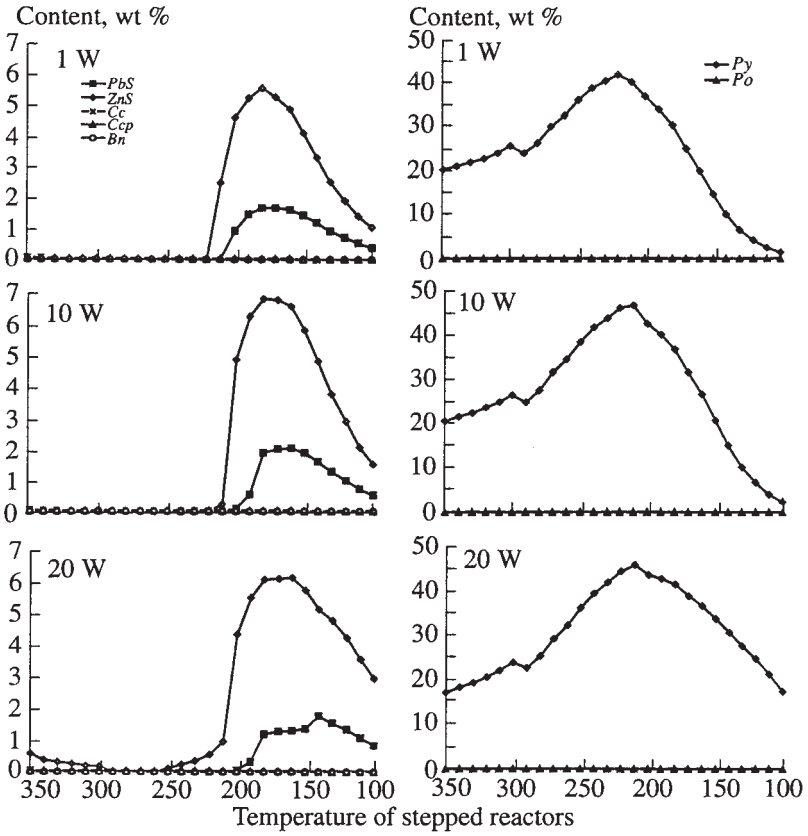

Fig. 73. Ore formation model VL4 (in the mobilization zone 370°C, 1 kbar, 10 kg of the Kholst granite with an elevated sulfur content). The structure of the filling vein at waves 1, 10, and 20 (initial metalliferous solution in Fig. 72). Quartz is not shown in the right-hand plots, with the content of this mineral complementary to 100%.

shifted toward higher temperatures (100–200°C in VL, 100–250°C in RL-5 layers, 220–240°C in VR); (2) the low-temperature field of sphalerite predominance expands (VL and RL-5 layers are dominated by galena alone, RL-10 layers at 100–150°C is dominated by sphalerite, and in VR sphalerite predominates over the interval of 100–200°C); (3) galena and sphalerite are absent at any temperatures only in RL models; and (4) in the models with mechanism of vein formation close to the layer mechanism, pyrite is precipitated simultaneously with the bulk of galena and sphalerite, i.e., at temperatures of 150–200°C (an increase in the role of the reaction mechanism results in an increase in the pyrrhotite fraction at low temperatures).

The inner structures of discrete updip segments of the veins clearly demonstrate the following regularities (some data are for the cross section through the model vein at 200°C in Fig. 77): (1) models close to the layer models (VL and RL-5 layers) display the absence of high sphalerite and galena concentrations near the selvages; (2) VL and RL models have some maxima of galena and sphalerite deposition, and an increase in the role of the reaction mechanism brings about a tendency toward the expansion of the region with the simultaneous crystallization of these sulfides at any temperatures; (3) the maximum of galena precipitation is shifted relative to the sphalerite maximum toward the inner parts of the model veins (VL and RL), i.e., sphalerite is massively deposited earlier than galena is; (4) the central portions of the veins (VL, RL) consist of quartz, and their selvages consist of quartz with pyrite or pyrrhotite, up to 2–3% sphalerite and up to 1% galena; and (5) the structure of the vein produced by the purely reaction mechanism reflects the uniform filling of the fracture conduit, with the differences between the mineral assemblages caused only by the time (wave) and temperature (updip level).

6.2.3. Comparison of the simulation results with factual data and their discussion

Our calculations allowed us to construct a series of models with different input or output parameters. The most realistic of them can be selected by comparing the results of modeling with factual data on the mineralogy and geochemistry of natural objects. Of course, when devising numerous models, we not only tried to achieve the closest similarity with natural prototypes, but we also analyzed the effects of the diversity of factors on the evolution of events during ore formation processes and, eventually, on the development of an orebody.

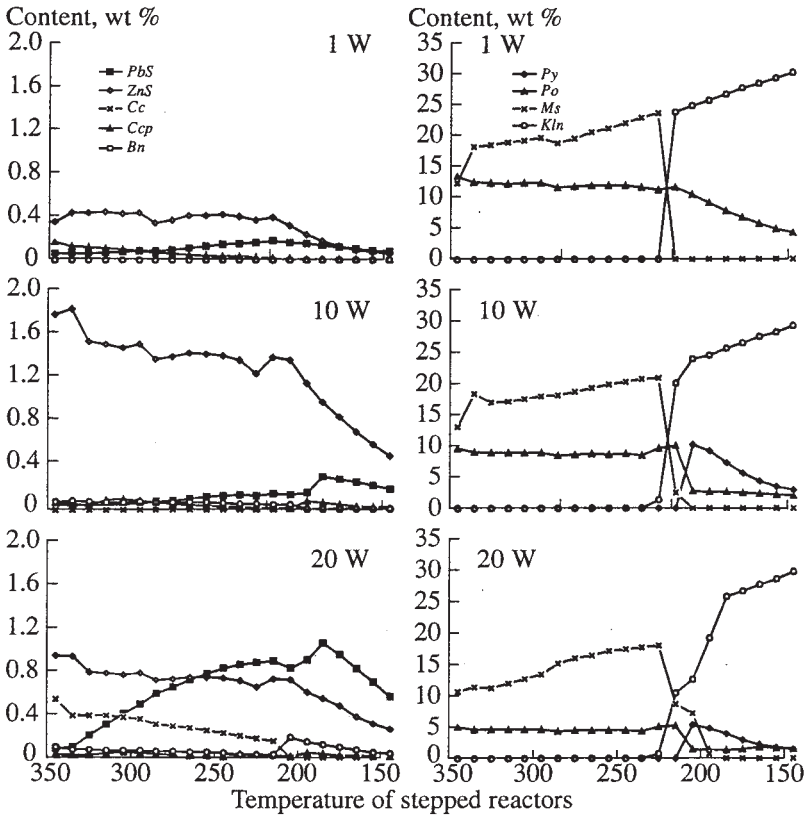

Fig. 74. Layer model VL6 of ore formation (0.1 g of granitic material in each reactor at each wave). The structure of the filling vein at waves 1, 10, and 20 (the initial metalliferous solution is analogous to that in model VL2, Fig. 64). Quartz is not shown in the right-hand plots, with the content of this mineral complementary to 100%.

(1) The main result of our simulations is the conclusion that the assumed structure of the models and simulation techniques, i.e., a combination of the mobilization zone and the region where veins develop (Fig. 61), can adequately describe the formation of orebodies that are analogous to quartz veins with base-metal ore mineralization at the Sadon group of deposits. Before constructing the models, we referred to the solutions that leached ore components from the mobilization zone as *potentially mineralized (metalliferous)*. Our models demonstrate that these solutions can transport ore elements and sulfide sulfur in concentrations sufficient for the development of ore minerals in veins, as well as silica, iron, and other major components of vein minerals with realistic proportions of the concentrations of these components.

(2) The development of mineralized veins without redeposition or with partial redeposition (the "layer" and "reaction–layer" models) are the main mechanisms generating ore mineralization at the deposits, while the processes of intraore metasomatism (the reaction model) plays a subordinate role (although these processes are widespread at the deposits, particularly in relation to sphalerite formation). The latter conclusion is accepted by most researchers of the deposits by virtue of mineralogical evidence. However, it is only our models that demonstrate how the vein material evolves and how variations in the external conditions (temperature, pressure, and the composition of the source granite) can affect the formation of minerals in veins. The results obtained with the layer and reaction–layer models for the recycling of a small number of layers are consistent with natural observations about an increase in the Pb/Zn ratio from the lower to upper portions of the veins and data on the "stages" of mineralization, principal regularities in the distributions of elements, and the temperatures at which ore minerals start to precipitate. All of these considerations were mentioned above when the choice of the layer model was justified as the main mechanism of the origin of the veins (see 1 in Section 6.2.2).

(3) Now consider more closely the quantitative proportions of minerals in veins at Zgid, Kholst, and other deposits of the Sadon group.

Galena and sphalerite are unequally distributed in natural veins, and their contents vary within broad limits, from trace concentrations to 19–20% (and, occasionally, even as high as 40%), but the average values for Pb and Zn in composite samples are usually 4–5% [Khetagurov *et al.*, 1992]. Analogous contents of sphalerite and galena were yielded by our models for the final stages of vein formation in the region where

the bulk of Pb and Zn is deposited (4–6% at waves 15–20 in models VL1, VL2, VL2p, and others, see Figs. 62, 65, and 66).

The results of other models make it possible to predict the conditions under which higher concentrations can be produced. For example, a pressure decrease (to 600 bar in model VL10, Fig. 67) or a temperature increase (to 440°C in model VL3, Fig. 70) in the mobilization zone brings about the development of very rich sphalerite–pyrite ores (from 12 to 35% ZnS and up to 50–70% pyrite) in the veins. Both a decrease in the pressure (to 600 bar in the models) and an increase in the temperature (to 440°C in the models) are highly probable in nature and were identified at the deposits by studying fluid inclusions [Lyakhov *et al.*, 1994]. No such increase in the galena concentration was noted in our models. However, there could be another cause of such extremely high sphalerite and galena concentrations in natural veins: metasomatism within these veins, a process that should inevitably follow tectonic reactivation and periodic fracturing of the vein mineral assemblages. Pyrite corrosion by sphalerite and galena or sphalerite corrosion by galena were described by many researchers at these deposits. These reactions lead to the almost complete deposition of ore elements and can result in fairly high galena and sphalerite concentrations. Such events ubiquitously occur in our simulations in compliance with the reaction model (Figs. 63 and 77).

In all models considered above, sphalerite deposition predates massive galena crystallization. This is typical of all deposits in the Sadon ore field [Chernitsin, 1962, 1985] and follows from indications that sulfides (sphalerite, pyrite, and pyrrhotite) were redeposited during galena crystallization.

Pyrite and pyrrhotite are the most widespread vein minerals (along with quartz) of mineralized veins at the deposits. Their contents in the veins vary from a few percent to 70% and, occasionally, even more. The values of 10–30% can be considered average.

Analogous pyrite and pyrrhotite contents were yielded by practically all of our models. A sharp increase in the pyrite or pyrrhotite content can occur early in the process of some model veins formation (at waves 1–5) and in models with a high-temperature leaching zone (up to 70% in model VL3 during a few first waves of the process of vein formation). It is quite probable that numerous pyrrhotite (quartz–pyrrhotite) veins at the Sadon deposit also affiliate with this type. These veins predate the main base-metal mineral stage at the deposit.

As follows from our models, the early evolutionary stages of the hydrothermal system can be marked by the development of veins of predominantly quartz–pyrrhotite or quartz–pyrite composition without base metals or with their low concentrations in the splay fractures of the main ore-hosting structures. These fractures could be cut off from the later mineralizing processes by premineral tectonic motions and, thus, were not replaced by younger mineral assemblages.

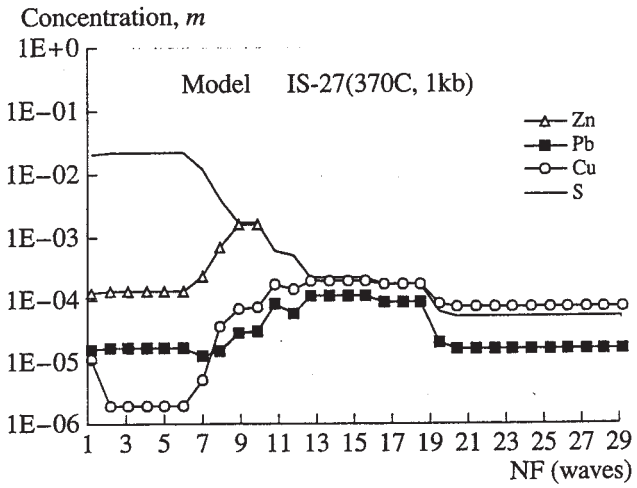

Fig. 75. Initial metalliferous solution of ore-formation model VL9. Variations in the concentrations (logarithm of molality) of ore elements and sulfide sulfur in the metalliferous solution as functions of the number of the portion of the primary solution (wave).

The deposits of this district are characterized by an increase in the pyrite/pyrrhotite ratio from lower to upper levels. This tendency was noted only in our models that are close to the layer type.

Among *Cu sulfides*, *chalcopyrite* is the most widespread mineral of the deposits, and its content usually ranges from 0.4 to 2.6% of the overall vein mass [Khetagurov *et al.*, 1992]. Bornite and chalcocite were also found in natural veins, but they usually replace chalcopyrite and their contents are very low. The overall concentrations of Cu sulfides in our models are as a rule consistent with factual data (these values for model veins commonly do not exceed 0.5–1.2% and occasionally reach as high as 1.6%). The early stages of vein formation (waves 1–5) are always marked by chalcopyrite precipitation (in amounts of 0.2–0.5%). Later, the metalliferous solutions in model veins deposit bornite (up to 1–1.2%, for example, in model VL1, Fig. 62), which is often followed by chalcocite (up to 0.6%, for example, in model VL2, Fig. 65) during the final stages of the process. It should be emphasized that neither bornite nor chalcosine replace chalcopyrite in purely layer models but, instead, are deposited from the solutions. Even in these situations at low temperatures, galena and sphalerite crystallize together with chalcopyrite (as at wave 20 in model VL1) or, occasionally, bornite (for instance, at wave 20 in model VL2). This also applies to the reaction–layer models.

Bornite (chalcocite), but not chalcopyrite, are formed because of a deficit in sulfide sulfur in the solution. This is obvious from the appearance of pyrrhotite in place of pyrite in model veins.

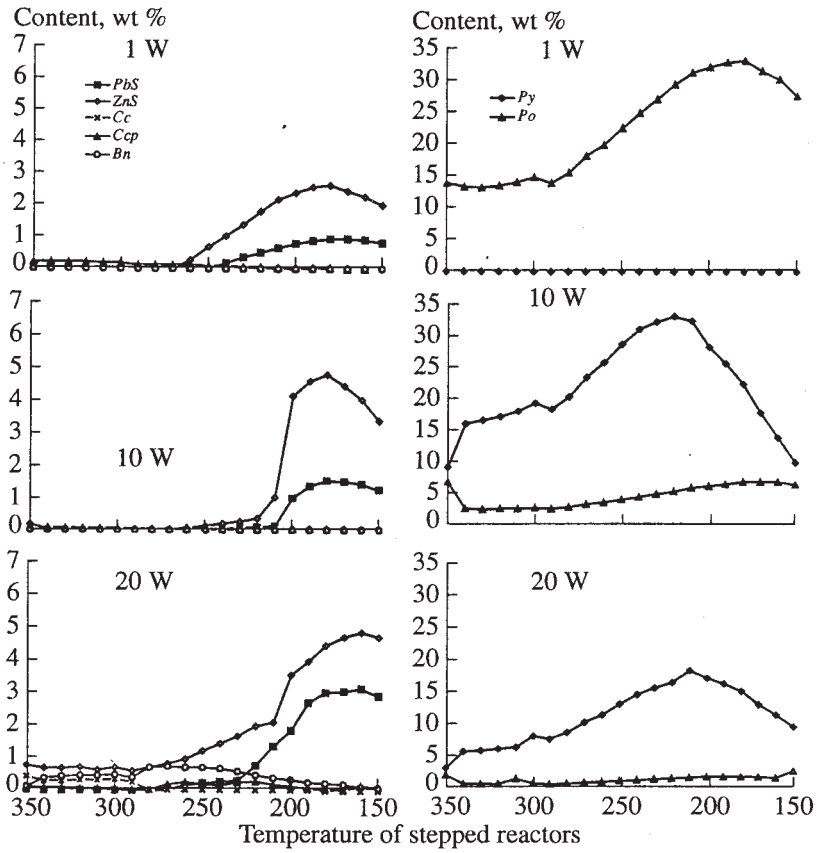

Fig. 76. Ore formation model VL9. The structure of the filling vein at waves 1, 10, and 20 (the composition of the initial metalliferous solution is shown in Fig. 75). Quartz is not shown in the right-hand plots, with the content of this mineral complementary to 100%.

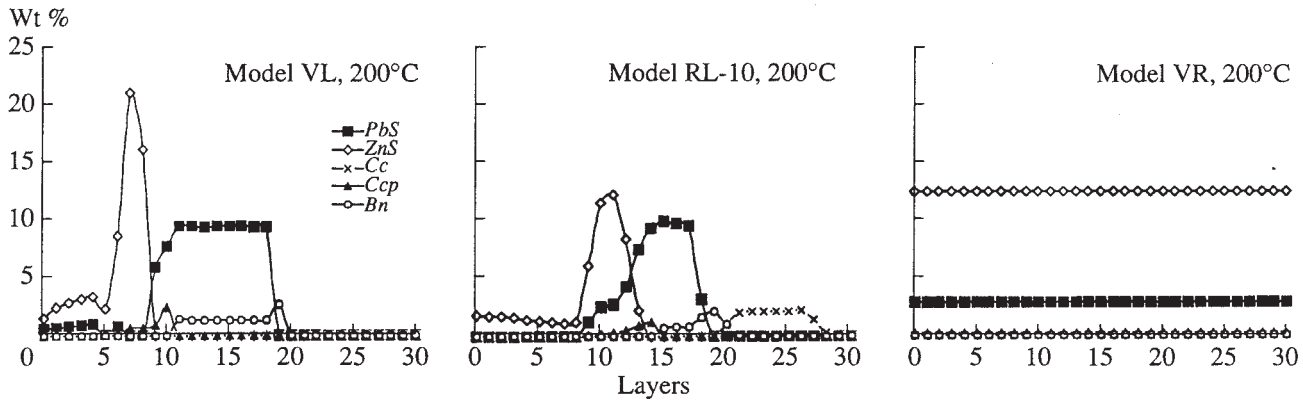

Fig. 77. Structure (cross sections) of model filling veins at wave 30 at a level corresponding to 200°C updip the vein (only ore sulfides are shown): the layer and reaction–layer mechanisms (RL-10 layers) and the reaction mechanism. The cross section runs from the vein selvage to its core (or the other selvage), i.e., between layers 0 and 30.

There can be more than one way to settle the problem of sulfur deficit during the origin of chalcopyrite alone, as is the case with some natural orebodies: some amounts of sulfide sulfur comes into the system with the primary solution (leaching model IS-3 with H_2S = 0.001 *m*, Fig. 58); the sulfur concentration in the pristine rock can be somewhat higher (model VL4, Fig. 73); and chalcopyrite can precipitate as a consequence of reaction with the early pyrrhotite or pyrite. The latter scenario seems to be the most realistic, because it is not necessary for the model to be stretched and is this confirmed by factual data. Reac-

tions of this type are well pronounced in the calculation results conducted for the reaction mechanism producing vein mineral assemblages: a deposition peak of sphalerite (up to 9%), galena (up to 8%), and chalcopyrite (up to 1.6%) at the boundary of pyrite reaction transformation (waves 15–20 in model VR1, Fig. 63).

Chlorite is a widespread vein mineral at the Sadon deposits. The contents of this mineral usually do not exceed 5–15% [Khetagurov *et al.*, 1992], although some veins contain quartz–chlorite aggregates with as much as 15–20% chlorite or perhaps even more (as in the Vostochnaya Vein at level VI of Verkhnii Zgid). None of our models shows more than 0.5% chlorite deposited from the hydrothermal solution together with other minerals. This is quite understandable, because the Al and Mg concentrations of the model solutions are very low ($n \times 10^{-5}$ *m* at 350°C), although the same solutions contain enough Si and Fe (~$n \times 10^{-2}$ and ~$n \times 10^{-3}$ *m*, respectively). We attacked the problem of chlorite proceeding from the concept that this mineral is formed metasomatically by the interaction of metalliferous solutions with the crushed and pulverized material of the wall rocks of the shear fractures that contained some alumina. Fragments of strongly altered country rocks are ubiquitously found in veins at the deposits.

Our calculation results demonstrate that chlorite could be formed in compliance with this mechanism. In model VL7, the early evolutionary stages of the vein are marked by the precipitation of as much as 10% Fe-chlorite (daphnite) in the near absence of Fe–Mg chlorite. Later in the course of vein evolution, the proportion of Fe- and Mg-chlorite in the model changes (mostly in the high-temperature region of 350–240°C). Very similar proportions of vein chlorites were documented by Zlatogurskaya [1960] at the Verkhnii Zgid deposit, where the first-generation early chlorite was identified as afrosiderite and the younger Fe–Mg chlorite belongs to ripidolite. It follows that our calculation data are compatible with natural observations not only in terms of the amounts of the chlorites but also in their chemistry. However, these processes producing chlorites are of local character and do not significantly affect the genesis of ore mineralization. There are many causes of this phenomenon: the unequal filling of the fractures with clastic material that can be only locally provided for these processes; the absence of the fine fraction of the clastic material fully prevents chlorite crystallization (as can be seen from the results of model VL6 and as has been observed in veins carrying large wall-rock fragments); and, finally, the character of ore deposition in the presence of chlorites is notably different from the general tendencies established for natural veins (this pertains to the deposition temperatures and the Pb/Zn ratio). Furthermore, the models demonstrate that chlorite formation is coupled with the deposition of up to 20–35% sericite, which, however, is not a typical or widespread vein mineral in orebodies at deposits of the Sadon group.

Another problem, which has not yet been settled in our models, is the origin of carbonates. *Carbonates* (calcite and Mn-siderite) are always formed in natural veins late in the course of their origin during all recognized stages of mineralization. However, our models yield no carbonates, which can be explained as follows. First, the solutions of our models are more acidic than is necessary for carbonate formation (as can be inferred from sericite or kaolinite crystallization during reactions with the clastic material in model VL6). Second, our model calculations were conducted for 20–30 waves (portions) of the solution and were mostly not carried up to the complete extraction of the base metals from the granite, i.e., until fully barren solutions started to ascend from the mobilization zone through fractures. Thus, it is quite possible that calcite will form in the model vein assemblages during later evolutionary stages.

(4) Calculations in some models were carried out for varying temperatures and pressures of the mobilization zone. Temperatures of approximately 400–420°C are yielded by fluid inclusions as the maximum values for the premineral evolutionary stage of the hydrothermal system. Moreover, schemes for the stages and temperature regime of the ore mineralization based on the microthermometry of fluid inclusions usually mark a number of intervals in which the temperature sharply increases and then monotonously decreases toward the end of the stage [Lyakhov *et al.*, 1994]. Jumps of this type commonly correlate with the boundaries between stages of mineral formation and with the most significant inter- or intrastage tectonic motions.

The microthermometry of fluid inclusions in minerals from deposits of the Sadon group indicates that the paleothermal fields of the ore mineralization were characterized by clearly pronounced temperature and pressure gradients, with the vertical gradients varying from 12 to 22°C or, occasionally, even up to 35°C and 11.4–24.5 MPa per 100 m [Lyakhov *et al.*, 1978, 1994; Laz'ko *et al.*, 1981]. These figures were cited above and were used to specify the temperature intervals in the models and possible pressure variations. These values also provide a rough idea about the linear dimensions of the model constructions. For example, the standard temperature interval of 350 to 100–150°C considered in the models can be correlated with a 800-m vein interval (at a gradient of 20–25°C). The selected temperature step of 10°C corresponds to ~20 m.

Three of the models analyze the effect of temperature variations in the mobilization zone on the character of mineral formation in the vein (440°C in model VL3, 370°C in VL2, and 320°C in VL5). Some of the simulation results have already been discussed in the context of the quantitative proportions of minerals. These data can also be utilized in analyzing the lateral zoning of the model vein body if the aforementioned three models are arranged along the temperature decrease vector,

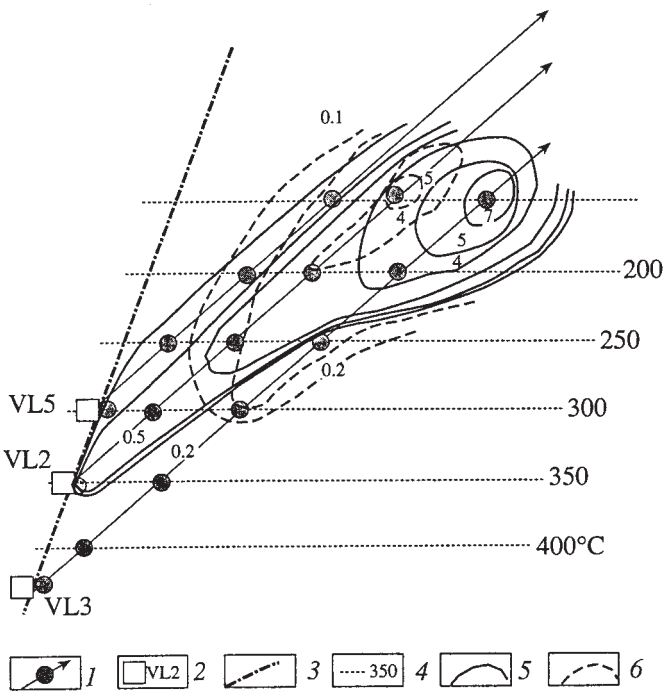

Fig. 78. Schematic cross section in the plane of the model vein body (constructed based on the results of calculations by models VL3, VL2, and VL5 for wave 20). (*1*) Calculated points and the line with an arrowhead indicates the trajectory and direction of the fluid flow in the fracture conduit; (*2*) model number and the position of the mobilization zone at the junction between a regional fault and its splay fracture array; (*3*) regional normal fault whose footwall contains the vein body; (*4*) temperature and the relative position of isotherms in the vein body plane during ore formation; (*5*) concentration isopleths for Zn (in wt % ZnS); (*6*) concentration isopleths for Pb (in wt % PbS).

i.e., when three trajectories of solution flows in the fracture plane are envisioned.

Figure 78 presents a schematic cross section of a situation of this type in the form of calculated isopleths of sphalerite and galena concentrations. In should be born in mind that mobilization zones seem to have much greater volumes than is shown in the scheme (these zones span both the junction zone itself and the wall rocks of the splay fracture structure).

Of course, this scheme is a generalization and idealization and does not take into account several complications that can also affect fluctuations in the ore material distribution (this can be an upward or downward shift of the mobilization zone with a given temperature, vertical pressure gradients, lateral temperature gradients, and the possible mixing of leaching solutions with different concentrations of some elements). However, the zoning pattern obtained for the distributions of elevated and anomalous Pb and Zn contents is in very good agreement with data on vein base-metal deposits: a vertical displacement of the concentrated deposition of galena relative to sphalerite and the transition from the quartz–galena–sphalerite to the quartz–sphalerite–galena assemblage away from the regional normal fault.

The same three models can be analyzed from the viewpoint of relative time, i.e., the stages of the hydrothermal process, when mobilization and ore deposition take place starting from 440°C, then lower temperature (for example, 370°C) processes affect the vein, after which the temperature can again increase or decrease. In this context, the calculation results should be regarded as alternating with the passage of time or "enclosed" in one another. Constructions of this kind are too abstract and complicated for a generalized model of ore genesis but seem to be quite realistic for an individual orebody.

Now consider models with a changing pressure. Model VL2p (Fig. 66), in which a temperature gradient is coupled with a pressure gradient (equal to ~250 bar per 100 m), does not exhibit any significant differences from the results of analogous model VL2 with a constant pressure. Because of this, we did not further complicate the system and carried out all later simulations for a constant pressure. It can be concluded that a pressure gradient does not play any significant role in ore-forming processes.

At the same time, the results of model VL10 (with a pressure in the mobilization zone of 600 bar, Fig. 67) demonstrate that a pressure decrease in the mobilization zone can have significant consequences (with all other parameters remaining the same). For example, the sphalerite concentration in the ores deposited during the early stages sharply increases (to 12–13% as compared to 3% in analogous model VL2 with a pressure of 1000 bar), and the pyrrhotite and pyrite contents also significantly increase (to 50–60% as compared to 20–30%). Peaks of this kind can, perhaps, take place during some evolutionary stages of the hydrothermal system.

(5) Our data make it possible to explain the stages of mineralization in the context of a continuous evolution of a single source of material, with interaction processes in the rock–water system playing a decisive role. Active intraore tectonics, which resulted in the periodically repeated fragmentation of preexisting mineral aggregates in the vein and in changes (expansion or diminishment) of the mobilization zone could, in turn, cause (depending on the temperature and pressure) partial repetition of earlier mineral-forming stages that overprinted older mineral assemblages and modified them (according to the reaction mechanism). Otherwise, the interrupted processes could resume again in compliance with the layer mechanism but under other starting conditions.

The estimated volume of granite needed to form a deposit with Pb and Zn reserves on the order of 100 thousand tons, provided the metals are completely extracted from the granite, is equal to approximately 0.6 km^3. This is quite a realistic figure, given that the deposits discussed here usually comprise dozens of

vein orebodies exposed over an area of dozens of square kilometers and extending for more than one kilometer updip.

6.2.4. Conclusions

The models discussed above led us to the following main conclusions.

(1) A structure of the model and simulation techniques were developed to model processes that produce vein base-metal ore mineralization because of a temperature decrease from the metal mobilization zone in granite to the region where orebodies develop in the granite.

(2) The development of mineralized veins without redeposition is the main mechanism generating ore mineralization with a subordinate role played by intraore metasomatic processes (which, nevertheless, are widespread at the deposits).

(3) Mineral stages can be caused by the evolution of a single source of ore material (which is, in our models, a zone of loosened rocks at the junction between a regional fault and its splay shear and detachment fractures), in which interactions in the rock–water system and their evolution with time played a decisive role.

(4) Equilibrium–dynamic modeling makes it possible to reproduce not only the principal structural features of the vein orebodies and the main regularities in the distributions of elements in them but also to obtain results that with high accuracy reproduce the quantitative and qualitative characteristics of natural mineral assemblages.

6.3. Models for the Development of Aureoles

Models for the development of quartz veins with base-metal ore mineralization remain incomplete until they involve processes leading to the origin of wall-rock aureoles of the distribution and redistribution of metals. The geochemical part of our research demonstrates that vein orebodies at the deposits are surrounded by infiltration-controlled aureoles of ore elements. These aureoles can be subdivided into three types: aureoles of deposition, redeposition, and leaching (see Chapter 5). We conducted a thermodynamic analysis of the processes generating these aureoles. Deposition–redeposition aureoles are the final element in the sequence mobilization zone → vein → aureole of our models. Conversely, mobilization aureoles (which were discussed above) are the first element of the sequence, as a result of which we begin our analysis of all physicochemical events.

6.3.1. Simulation methods and conditions

Simulation techniques applicable to deposition–redeposition and leaching aureoles are different and thus will be described separately.

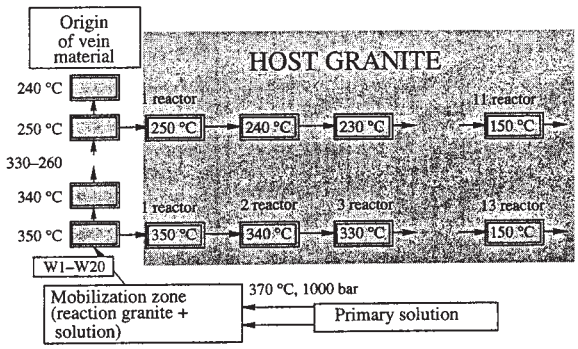

Fig. 79. Modeling scheme and model structures for the zone where deposition–redeposition aureoles develop. *W* are portions (waves) of solution from the mobilization zone; they are analogous to NF in Section 6.1.

Deposition–redeposition aureoles. The model of an aureole in the simulations is represented by 11–13 consecutive flow-through reactors (Fig. 79).

The number of reactors and the temperature distribution between them are determined by the initial temperature, step of temperature changes, and the assumed final temperature.

The generalized scheme of simulation is fairly simple (Fig. 79). The solution from the mobilization zone enters into a fracture conduit, in which the solution precipitates (or does not precipitate) vein minerals. Simultaneously (or subsequently), some mass of the solution that was in equilibrium with the vein material can penetrate into (filter through) the wall rocks (granite). This solution reacts with the wall rocks in the first reactor. The solution equilibrated with the rock in reactor 1 flows to rector 2 and so on up to the last reactor in question. The transformation of the solution that leaves the last reactor is usually not considered.

Hence, the models of aureoles of this type are rigidly related (in terms of *T*, *P*, and the composition of the solutions) to the models for the development of vein bodies, and we calculate the whole succession of interaction in the solution–rock system starting from the mobilization zone, through the vein, and to the aureole. The overall number of reactors varies. For example, if the simulated aureole has an initial temperature of 350°C, the sequence of calculations in as follows: mobilization zone (370°C)—one reactor, zone of vein development (350°C)—one reactor, zone of aureole development (350–150°C)—13 reactors, i.e., 15 sequential flow-through reactors. If the simulated aureole has an initial temperature of 250°C, the sequence of calculations is different: mobilization zone (370°C)—one reactor, zone of vein development (350–250°C)—11 reactors, zone of aureole development (250–150°C)—11 reactors i.e., 23 sequential flow-through reactors (see Fig. 79). The succession of reactors is passed by 20–30 sequential portions (waves) of solutions from the mobilization zone.